A PASSIVE-ADAPTIVE WING FOR DRAG REDUCTION.

C. B. York*, Y.B. Murta, S.F.M Almeida*****
***University of Glasgow, **Embraer, ***University of Sao Paulo**

Keywords: *Laminate Tailoring, Extension-Shearing coupling, Bending-Twisting coupling Passive-Adaptive Design.*

Abstract

This article presents details of the development of a passive-adaptive composite wing design for future wind tunnel drag measurements. Simulations of static tests are performed on a composite wing-box to assess the effect of imposing standard manufacturing constraints, such as ply percentages, ply contiguity and ply orientations on the laminate skin panels, which must possess extension-shearing coupling. This form of coupling is achieved through the use of standard ply orientations aligned with the structural axis and with off-axis alignment. The latter is also applied to double angle-ply laminates. All designs are compared to isotropic (datum) laminate skin panels to assess the relative bending-twisting coupling performance of the wing box.

1 Introduction

The latest research on the application of lightweight materials in reducing aircraft fuel burn [1] indicates that if the average empty weight of an aircraft could be reduced by 10%, the fuel burn would be reduced by 7%. However, if this weight saving could be traded for increased wing aspect ratio, and the aerodynamic efficiency that this brings, the fuel saving would be leveraged by a factor of 2 to 3, i.e., to between 14 and 22%.

Aero-elastic tailoring of composite wings may lead to a valuable drag reduction mechanism in conventional swept back wings [2]. This can be achieved by introducing passive bending-twisting coupling behaviour (a so called passive-adaptive wing), to maintain a constant angle of attack across the wing, irrespective of the magnitude of the bending deflections. Drag increases in conventional swept back wings with any fluctuation away from the optimized static cruise configuration, i.e., whenever the wing twists differentially as it bends. The effect on aircraft fuel burn, of eliminating this drag penalty, has not been quantified in the open literature.

A significant step change in fuel burn efficiency is, however, likely to come about only from the adoption of more radical designs, such as forward swept wings, which are well known for their aerodynamic superiority over conventional swept back wings. Nevertheless, the problem of aerodynamic divergence has remained a barrier to more widespread use, despite predictions that aero-elastically tailored composite wings will overcome this problem, even at relatively high aspect ratio [3]. Only low aspect ratio wings have so far been developed for flight trials, e.g. the iconic X-29 demonstrator aircraft.

The prospect of high aspect ratio forward swept wings may now be on the horizon as a result of the EU-FP7 funded ALaSCA [4] project (Advanced Lattice Structures for Composite Airframes), where the optimised aircraft configuration, consisting of a long geodesically stiffened fuselage barrel section [5], claimed to achieve a 25% reduction in mass compared to tradition fuselage construction, is necessarily mounted ahead of a forward swept wing, with aft fuselage mounted engines, see Fig. 1. This design concept arises from the DLR funded LamAiR project, demonstrating laminar airflow wing technology in forward swept wings. The merits of these composite airframe projects have led to the follow-on EU-FP7 funded PoLaRBEAR [6] project (Production and

Analysis Evolution for Lattice Related Barrel Elements under Operations with Advanced Robustness), but attention has not yet focused on the structural flexibility issues associated with high aspect ratio forward swept wings.

Fig. 1 – The ALaSCA EU FP7 funded project on Advanced Lattice Structures for Composite Airframes using an aircraft configuration consisting of a long fuselage barrel section mounted ahead of a high aspect ratio forward swept wing, with aft fuselage mounted engines.

2 Wing design

Passive-adaptive wings can achieved by introducing mechanical Extension-Shearing coupling in the wing skins [10]. Isotropic composite wing skins are also developed as a datum, against which the influence of laminate tailoring strategies are assessed through Finite Element Analysis (FEA) simulations; final designs are currently being validated through static testing.

A passive-adaptive composite (NACA 0012) wing will be developed for future wind tunnel drag measurements. Hence simulations are performed here to assess the effect of imposing standard manufacturing constraints, such as ply percentages, ply contiguity and ply orientations on the laminate skin panels, as well as unconventional laminate designs, which will possess *Extension-Shearing* coupling. However, the associated manufacturing uncertainties are difficult to capture through simulation alone, hence static tests are currently being performed to demonstrate that stiffness and strength characteristics are met prior to wind-tunnel testing.

2.1 Manufacturing considerations

Scaled flexible wind-tunnel models present a manufacturing challenge. A semi-monocoque wing-box profile must usually be constructed in parts, to satisfy the requirements for passive adaptive designs, which have discontinuous ply orientations between the top and bottom surfaces of the wing-box, such that a standard filament winding process cannot be adopted. However, the necessary construction joints in the wing-box are now sites of aerodynamic disturbance which will significantly affect the planned drag measurements at a later stage of the project. Therefore, to achieve an aerodynamically smooth surface profile, a novel approach to mitigating the effects of construction joints is required, using the concept of a thin-ply laminate preform. The preform will be wrapped around a male tool, which is sheathed in an inflatable bladder, then placed inside a female tool, forming the outer mould line of the wing-box profile, and the bladder inflated under high pressure to achieve consolidation of the composite material during autoclave curing. The thin-ply preform constitutes a novel approach, involving termination of angle plies around the leading edge of the wing-box profile, to meet the requirement for different ply orientations in the top and bottom surfaces. This approach also provides a flexible hinge at the leading edge, allowing an internal spar/rib structure to be inserted through the un-bonded trailing edge of the wing-box, post cure.

The emergence of thin ply composite material, consisting of either non-crimp fabrics (two or three layers of uni-directional material stitched through their thickness) or woven cloth with very low crimp, using spread tow manufacturing technology, introduces a game changing opportunity; not only do these materials bring design flexibilities found only in thick laminate construction into the thin laminate domain, but the design rules for traditional uni-directional materials are no longer generally applicable. The design space of these novel laminates, with thin-ply material architures, have been derived algorithmically [13]-[15], identifying the properties necessary to develop the desired mechanical coupling behaviour, but with immunity to thermal warping distortion, i.e., thermal coupling behaviour, that generally occurs after a high temperature curing process. Passive adaptive behaviour could not be achieved in scaled flexible wing-tunnel models

without the adoption of thin ply composite materials.

A prismatic section represents a substantial simplification, since it ignores many practical design considerations such as taper of the wing box cross section and skin thickness taper (through ply terminations), leading to changes in stiffness and coupling characteristics. However, the goal of the current study is to understand the performance of competing composite wing skin designs in order to inform the manufacture of a passive adaptive wing for future wind tunnel testing.

2.2 Laminate design

The development of a passive adaptive *Bending-Twisting* coupled wing requires E*xtension-Shearing* coupled laminate skins, as detailed elsewhere [10]. The necessary mechanical properties can be achieved in a number of ways, hence the following section describes competing design strategies, based on: (1) off-axis alignment of otherwise balanced and symmetric laminates with standard ply orientations (0°, ±45° and 90°); (2) off-axis orientation of double angle-ply (±ϕ° and ±ψ°) laminates, with otherwise *Uncoupled* properties and; (3) *Extension-Shearing* coupled (only) laminates with standard ply orientations. An isotropic laminate configuration with standard ply orientations is also used to provide a datum against which the coupled designs can be assessed. This necessarily fixes the designs to 24 ply laminates, representing the minimum ply number grouping for $\pi/4$ isotropy. The corresponding stacking sequence is:

$$[45/90/0/-45/0/-45/90/-45/45/0/45/90/45/90/-45/90/0/45/0/-45/0/-45/45/90]_T \quad (1)$$

The (non-symmetric) isotropic laminate was developed in a previous study on Non-Crimp Fabric (NCF) architectures for improved deposition rate [11], but of course can be manufactured using UD material, which is a requirement for the *Extension-Shearing* coupling only designs, which cannot be achieved with NCF for this ply number group.

For the first laminate class, balanced and symmetric designs can be extracted from databases containing fully *Uncoupled* [12] and/or *Bending-Twisting* [9] coupled laminates. Here, only *Uncoupled* balanced and symmetric solutions are extracted, despite the fact that they represent only a small fraction of the available design space.

A lamination parameter point cloud, representing the extensional stiffness properties of 39 unique designs with fully *Uncoupled* stiffness properties, is illustrated in Fig. 2. Ply percentages for standard ply orientations are superimposed on the lamination parameter design space, since these are commonly used in design practice. Typical aircraft components are provided for reference, with ply percentages in parentheses for 0°, ±45° and 90° orientations, respectively:

1. Spar (10/80/10),
2. Skin (44/44/12) and
3. Stiffener (60/30/10).

The ply percentages correspond to the equivalent in-plane lamination parameters (ξ_1, ξ_2):

1. Spar (0, -0.6),
2. Skin (0.32, 0.12) and
3. Stiffener (0.5, 0.4)

All points represent fully *Uncoupled* balanced and symmetric laminates within the 10% design rule and with a ply contiguity constraint of no more than 3 adjacent plies with identical orientation.

Elements of the extensional stiffness matrix [**A**] are related to the lamination parameter coordinates of Fig. 2 by:

$$\begin{aligned}
A_{11} &= \{U_1 + \xi_1 U_2 + \xi_2 U_3\} \times H \\
A_{12} = A_{21} &= \{-\xi_2 U_3 + U_4\} \times H \\
A_{16} = A_{61} &= \{\xi_3 U_2/2 + \xi_4 U_3\} \times H \\
A_{22} &= \{U_1 - \xi_1 U_2 + \xi_2 U_3\} \times H \\
A_{26} = A_{62} &= \{\xi_3 U_2/2 - \xi_4 U_3\} \times H \\
A_{66} &= \{-\xi_2 U_3 + U_5\} \times H
\end{aligned} \quad (1)$$

where $\xi_3 = \xi_4 = 0$ for *Uncoupled* designs, H is the total laminate thickness and the laminate invariants:

$$\begin{aligned}
U_1 &= \{3Q_{11} + 3Q_{22} + 2Q_{12} + 4Q_{66}\}/8 \\
U_2 &= \{Q_{11} - Q_{22}\}/2 \\
U_3 &= \{Q_{11} + Q_{22} - 2Q_{12} - 4Q_{66}\}/8 \\
U_4 &= \{Q_{11} + Q_{22} + 6Q_{12} - 4Q_{66}\}/8 \\
U_5 &= \{Q_{11} + Q_{22} - 2Q_{12} + 4Q_{66}\}/8
\end{aligned} \quad (2)$$

which are given in terms of the reduced stiffnesses:

$$Q_{11} = E_1/(1 - \nu_{12}\nu_{21})$$
$$Q_{12} = \nu_{12}E_2/(1 - \nu_{12}\nu_{21}) \quad (3)$$
$$Q_{22} = E_2/(1 - \nu_{12}\nu_{21})$$
$$Q_{66} = G_{12}$$

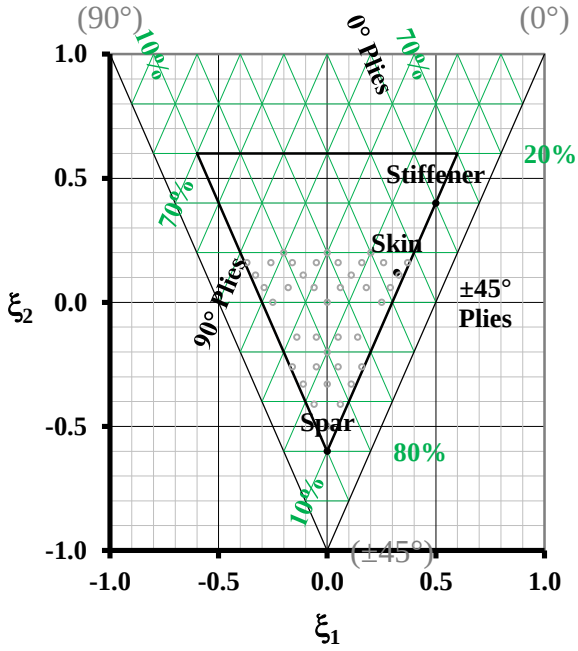

Fig. 2 – Lamination parameter design space for extensional stiffness of *Uncoupled* balanced and symmetric laminates, including typical Spar, Skin and Stiffener components, with superimposed ply percentage mapping.

An off-axis orientation (β°) sweep is now performed on the designs of Fig. 2, including typical skin panel designs, which are of primary interest in this study. Off-axis orientation gives rise to *Extension-Shearing* coupling, since $\xi_3, \xi_4 \neq 0$. This result can be compared to the maximum hypothetical result for standard orientations, within the bounds of the 10% rule, which corresponds to $(\xi_1, \xi_2, \xi_3) = (0, -0.6, \pm 0.6)$, and a value of $A_{16}/A_{11} = 39.8\%$.

For the second class of laminate with double angle-ply configurations, a new design methodology is adopted for matching bending stiffness, hence initial buckling strength [16], between standard ply laminates (with 0°, ±45° and 90° ply orientations) and double angle-ply laminates (with ±ψ and ±ϕ ply orientations).

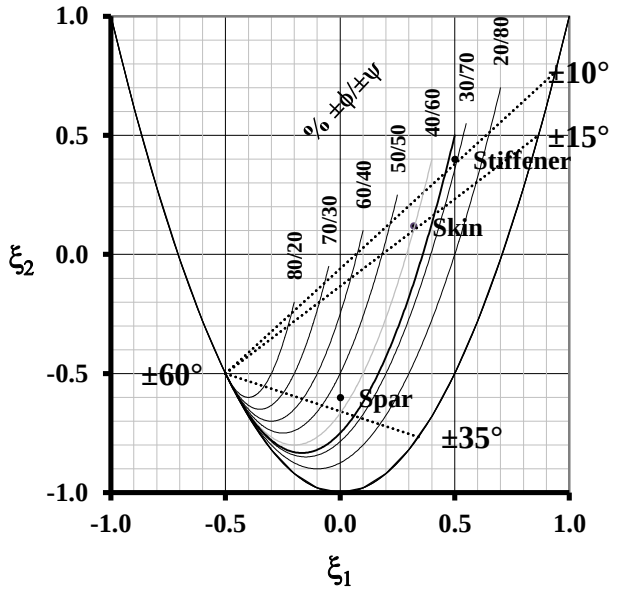

Fig. 3 – Lamination parameter design space for uncoupled extensional stiffness matching between typical Spar, Skin and Stiffener components, using double angle-ply designs with hypothetical ply percentages (±ϕ/±ψ). The solid line represents the 24 layer double angle-ply stacking sequence: $[\underline{\psi/-\psi/-\phi/\phi/-\psi/\psi/\phi/-\phi/\phi/-\phi/-\phi/\phi/-\phi/\phi/-\phi/\phi/-\psi/\psi/\phi/-\phi/\underline{\psi/-\psi}]_T$, with $\phi = 60°$ and $0° \leq \psi \leq 60°$.

This class of laminate has recently been shown to offer potential improvements in strength [17] and ease of manufacture [18]-[19] compared to standard ply laminates, but no consideration has yet been given to buckling strength, which becomes the critical design case towards the wing tip.

The methodology is only possible through the development of a series of databases containing laminate configurations with specific mechanical coupling characteristics. Results for 24 ply laminates, given in Fig. 3, demonstrate that the extensional stiffness requirements for a typical spar and stiffener can be closely matched by adopting a double angle-ply design with fixed (33.3/66.7) ply percentages, with $\pm\phi = \pm 60°$, representing a commercially available non-crimp fabric, and adjusting only the ply orientation, ±ψ, in the secondary angle-ply sub-laminate to give $(\pm\phi/\pm\psi =)$ ±60°/±10° for the stiffener and ±60°/±35° for the spar.

In this study, double angle-ply laminate are first designed to have isotropic bending stiffness. This allows off-axis alignment between the manufacturing and structural axes in order to introduce *Extension-Shearing* coupling, without

degrading the buckling performance, as would be the case for standard ply designs.

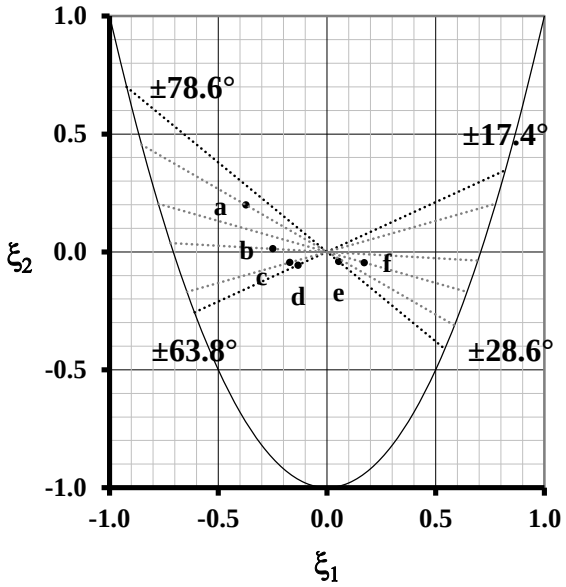

Fig. 4 – Lamination parameter design space representing extensional stiffness for 24 layer double angle-ply designs with Bending Isotropy, i.e. $\xi_9 - \xi_{12} = 0$.

Figure 3 demonstrates the variation in the in-plane properties (ξ_1, ξ_2) for stiffness matched laminates in bending; here, all possess bending isotropy. Broken lines drawn through the design points **d** and **e** intersect the parabolic bounds of the lamination parameter design space at (ϕ = 63.8°, ψ = 17.4°) and (ϕ = 78.6°, ψ = 28.6°), respectively. These represents the bounds on the range of 24 layer double angle-ply designs with bending isotropy, all of which are given in Table 1.

The third design case involves *Extension-Shearing* coupled (only) laminates with standard ply orientations. The maximum A_{16}/A_{11} = 16.2% and corresponds to the following stacking sequence, which shares the same compression buckling strength as the isotropic design, i.e., the classical buckling factor k_x = 4.00:

$$[-45/0/45/90/90/0/45/45/-45/45/90/45/45/90/45/-45/45/90/45/0/45/0/90/-45]_T \quad (2)$$

3 Wing-box simulations

This section demonstrates the potential performance of the competing laminate designs through simulation using a symmetric airfoil (NACA 0012) section, assuming the wing box is prismatic and of monocoque construction. The dimensions of the wing have been set to facilitate future wind tunnel experiments with a span of 1,500mm and chord length of 144mm. This gives a wing aspect ratio of above that of current metallic wing designs; a limitation due to flutter.

Simulations were generated with the ABAQUS finite element code [20] with a thin plate element (S4R5); a 24-ply laminate, of total thickness $H = (n \times t = 24 \times 0.062\text{mm} =)$ 1.488mm, ensures that this is representative of the thin plate solution. Material properties of the Graphite/Epoxy are assumed to represent T300/5208: E_1 = 181,000 N/mm^2, E_2 = 10,300 N/mm^2, G_{12} = 7,170 N/mm^2 and ν_{12} = 0.28.

A high degree of displacement convergence is achieved simply by adequately defining the NACA 0012 profile; in this case with an average element width of 1.5mm, corresponding to approximately 200 points for describing the profile:

$$\pm y = t/0.20 \times (0.29690x^{0.5} - 0.12600x - 0.35160x^2 + 0.28430x^3 - 0.10150x^4) \quad (3)$$

Table 1 – Stacking sequences for Uncoupled double angle-ply laminates with 24 layers together with angles (ϕ, ψ) which give bending isotropy. Off-axis alignment, β, corresponds to maximum *Extension-Shear* coupling (A_{16}/A_{11}).

	Stacking sequence	Bending Isotropy		*Extension-Shearing*	
		ϕ	ψ	β	(A_{16}/A_{11})
_*a*	$[\psi/-\psi/-\phi/\phi/\phi/-\phi/\phi/-\phi/-\phi/\phi/-\psi/\psi/-\psi/\psi/\phi/-\phi/-\phi/\phi/-\phi/\phi/\phi/-\phi/\psi/-\psi]_T$	63.78	17.44	32.5	-8.3%
b	$[\psi/-\psi/\phi/-\phi/-\phi/\phi/-\phi/\phi/-\psi/\psi/\phi/-\phi/\phi/-\phi/-\psi/\psi/-\phi/\phi/-\phi/\phi/\phi/-\phi/\psi/-\psi]_T$	65.08	19.58	33.8	-10.4%
c	$[\psi/-\psi/-\phi/\phi/\phi/-\phi/-\psi/\psi/\phi/-\phi/-\phi/\phi/\phi/-\phi/-\phi/\phi/-\psi/\psi/-\phi/\phi/\phi/-\phi/\psi/-\psi]_T$	68.06	23.04	38.3	-14.4%
d	$[\psi/-\psi/-\phi/\phi/-\psi/\psi/\phi/-\phi/\phi/-\phi/\phi/-\phi/-\phi/\phi/-\phi/\phi/-\phi/\phi/-\psi/\psi/\phi/-\phi/\psi/-\psi]_T$	74.28	27.06	46.1	-22.0%
e	$[\psi/-\psi/\phi/-\phi/-\phi/\phi/\psi/-\psi/-\psi/\psi/-\psi/\psi/-\psi/\psi/-\psi/\psi/\psi/-\psi/-\phi/\phi/\phi/-\phi/\psi/-\psi]_T$	70.46	24.95	56.2	10.0%
f	$[\psi/-\psi/\phi/-\phi/\psi/-\psi/-\phi/\phi/-\psi/\psi/-\psi/\psi/-\psi/\psi/-\psi/\psi/-\phi/\phi/\psi/-\psi/\phi/-\phi/\psi/-\psi]_T$	78.64	28.59	59.1	3.6%

with t = 0.12 for a NACA 0012 of zero camber, where t is the maximum thickness expressed as a fraction of the chord length.

A total of 11,800 elements are used to generate the wing. The wing root is fully built in and a tip load is applied to the profile such that the isotropic design has zero twist. This is achieved using a dummy node at the shear centre, which is rigidly connected to all perimeter nodes of the profile, acting as a rigid diaphragm. A linear analysis is employed for computation expedience, which is justifiable in this instance given that only the relative tip displacement and twist is being assessed.

4 Results and Discussion

Bending-Twisting coupling performance of the competing laminate designs are now assessed for the range of sweep angles, illustrated in Fig. 5, with constant planform area.

Simplified loading has been chosen to highlight the effects of the laminate coupling behaviour. Similarly, a prismatic wing box has been chosen to simply geometry and material properties, which are invariant along the span.

Only wing tip displacements and associated twist magnitudes are presented here.

Given the geometry and applied tip load, the twist angle will be maximum at the tip, therefore a zero twist at the tip implies zero twist across the span.

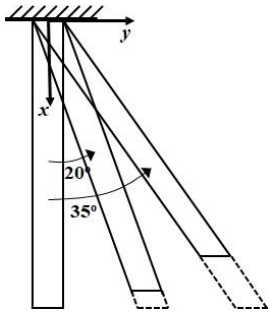

Fig. 5 – Illustration of sweep angle with constant wing area. Broken lines represent alternative wing geometry with the same projected span as the straight (0°) wing.

The isotropic wing has gradually increasing *Bending-Twisting* coupling with increasing sweep angle. For the special case of 35° sweep, the large jump in tip deflection and nose down twist from 0.58° to 0.73° degrees is proportional to the increase in span length, as illustrated in Fig. 6.

The *Extension-Shearing* (*E-S*) designs demonstrate a nose up tendency in the straight (0°) wing, which changes to nose down with increasing sweep angle. The *Hypothetical* maximum *Extension-Shearing* (*E-S-H*) has a lower axial stiffness, hence higher deflection

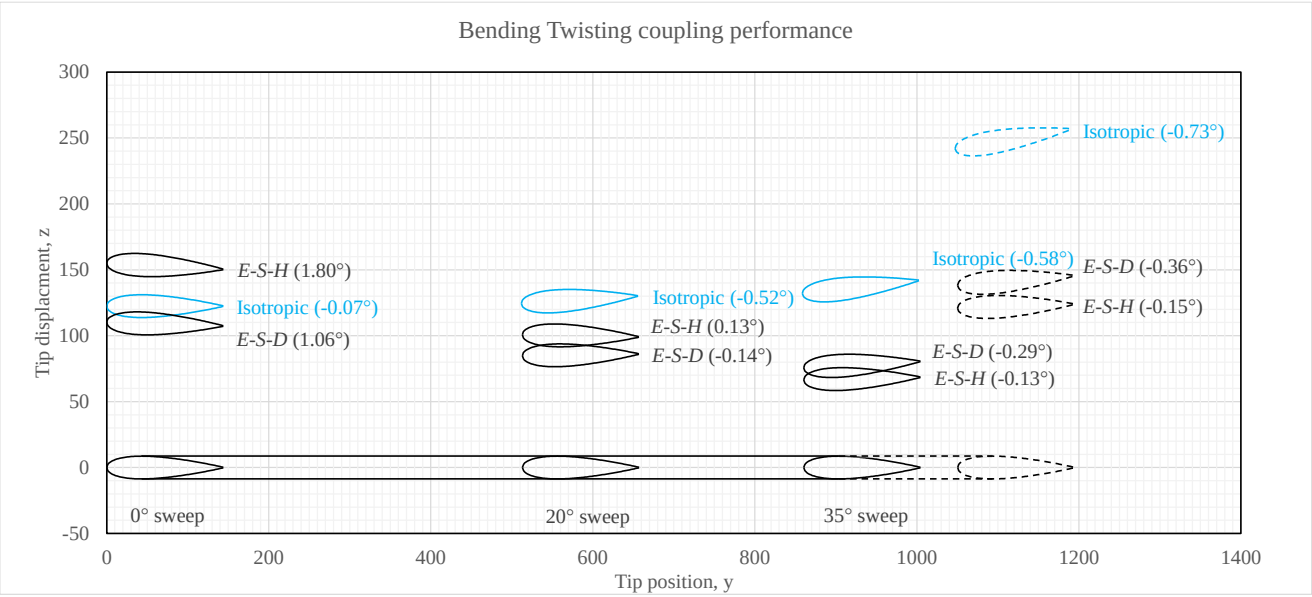

Fig. 6 – Relative wing tip displacement profiles (and twist angles, measure positive clockwise) for competing laminate designs with 0°, 20° and 35° sweep angles with constant wing area. Profiles illustrated with broken lines represent a special case of a 35° sweep angle with the same projected span as the straight (0°) wing. *E-S-H* profiles represent the maximum *Hypothetical Extension-Shearing* coupling design for standard ply orientations, whilst the *E-S-D* represent the *Double* angle-ply design with *Extension-Shearing* coupling.

than the *Double* angle-ply design (*E-S-D*). However this relationship is sweep angle dependent.

4 Conclusions

A number of laminate tailoring design approaches have been assessed.

Each design was selected for maximum laminate level *Extension-Shearing* coupling to prove the feasibility of the proposed passive adaptive wing design.

The results demonstrated that the phenomenon is sweep angle dependent, however in all cases, there is potential to achieve zero twist through the laminate tailoring strategies presented.

The work reported here is part of an ongoing project and will be made available via Enlighten, the open access repository at the University of Glasgow: http://eprints.gla.ac.uk/159763/

Acknowledgements

The first author gratefully acknowledges the support of the Engineering and Physical Sciences Research Council (EPSRC EP/S013555/1).

References

[1] Poll DIA. On the application of light weight materials to improve aircraft fuel burn – reduce weight or improve aerodynamic efficiency? *Aeronautical Journal*, Vol. 118, No. 1206, pp. 903 – 934, 2014.

[2] Jutte CV and Stanford BK. *Aeroelastic tailoring of transport aircraft wings: state-of-the-art and potential enabling technologies*. NASA/TM-2014-218525, 2014

[3] Weisshaar TA. Aeroelastic Tailoring of Forward Swept Composite Wings. *Journal of Aircraft*, Vol. 18, No. 8, pp. 669-676, 1981.

[4] http://cordis.europa.eu/result/rcn/149775_en.html

[5] Niemann S, Kolesnikov B, Lohse-Busch H, Hühne C, Querin OM, Toropov VV and Liu D. The use of topology optimization in the conceptual design of the next generation lattice composite aircraft fuselage structures. *Aeronautical Journal*, Vol. 117, No. 1197, pp. 1139-1154, 2013.

[6] http://cordis.europa.eu/project/rcn/111110_en.html

[7] York CB. New Insights into Stiffness Matching between Standard and Double Angle-ply Laminates. *Proc 11th Asian-Australian Conference on Composite Materials*, Cairns, Australia, 29 Jul - 01 Aug 2018.

[8] York CB and Almeida SFM. On extension-shearing bending-twisting coupled laminates. *Composite Structures*, Vol. 164, pp. 10-22, 2017.

[9] York CB. On bending-twisting coupled laminates. *Composite Structures*, Vol. 160, pp. 887-900, 2017.

[10] York CB. On extension-shearing coupled laminates. *Composite Structures*, Vol. 120, pp. 472-482, 2015.

[11] York CB and Almeida SFM. Tapered laminate designs for new non-crimp fabric architectures. *Composites Part A: Applied Science and Manufacturing*, Vol. 100, pp. 150-160, 2017.

[12] York CB. Characterization of non-symmetric forms of fully orthotropic laminates. Journal of Aircraft, Vol. 46, No. 4, pp. 1114-1125, 2009.

[13] Shamsudin MH and York CB. On Mechanically Coupled Tapered Laminates with Balanced Plain Weave and Non-Crimp Fabrics. *Proc 20th International Conference on Composite Materials*, Copenhagen, Denmark, 19-24 Jul 2015.

[14] York CB and Almeida SFM. Design Space Interrogation for New C-Ply Laminate Architectures. *Proc 17th European Conference on Composite Materials*, Munich, Germany, 26-30 June 2016

[15] York CB and Almeida SFM. Tapered laminate designs for new non-crimp fabric architectures. *Composites Part A: Applied Science and Manufacturing*, Vol. 100, pp. 150-160, 2017.

[16] York CB. New Insights into Stiffness Matching between Standard and Double Angle-ply Laminates. *Proc 11th Asian-Australian Conference on Composite Materials*, Cairns, Australia, 29 Jul - 01 Aug 2018.

[17] Tsai S. Keynote: Design of composite laminates. *Proc 21st International Conference on Composite Materials*, Xi'an, China, 20-25 Aug 2017.

[18] Nielsen MWD, Johnson KJ, Rhead AT and Butler R. Laminate design with non-standard ply angles for optimised in-plane performance. *Proc 21st International Conference on Composite Materials*, Xi'an, China, 20-25 Aug 2017.

[19] Nielsen MWD, Johnson KJ, Rhead AT and Butler R. Laminate design for optimised in-plane performance and ease of manufacture, Vol. 177, pp. 119-128, 2018.

[20] ABAQUS/Standard, Version 6.14. Dassault Systèmes Simulia Corp., 2014.

Copyright Statement